

RESEARCH

Open Access



Endothelial-mesenchymal crosstalk drives osteogenic differentiation of human osteoblasts through Notch signaling

Daria Perepletchikova¹, Polina Kuchur¹, Liubov Basovich¹, Irina Khvorova¹, Arseniy Lobov¹, Kseniia Azarkina¹, Nikolay Aksenov¹, Svetlana Bozhkova², Vitaliy Karelkin² and Anna Malashicheva^{1*}

Abstract

Background Angiogenesis and osteogenesis are closely interrelated. The interaction between endothelial and bone-forming cells, such as osteoblasts, is crucial for normal bone development and repair. Juxtacrine and paracrine mechanisms play key roles in cell differentiation towards the osteogenic direction, assuming the direct effect of endothelium on osteogenic differentiation. However, the mechanisms of this interplay have yet to be thoroughly studied.

Methods Isolated endothelial cells (EC) from human umbilical vein and human osteoblasts (OB) from the epiphysis of the femur or tibia were cultured in direct and indirect (separated by membrane) contact in vitro under the osteogenic differentiation conditions. Osteogenic differentiation was verified by RT-PCR, and alizarin red staining. Shotgun proteomics and RNA-sequencing were used to compare both EC and OB under different co-culture conditions to assess the mechanisms of EC-OB interplay. To verify the role of Notch signaling, experiments with Notch modulation in EC were performed by EC lentiviral transduction with further co-cultivation with OB. Additionally, the effect of Notch modulation in EC was assessed by RNA-sequencing.

Results EC have opposite effects on osteogenic differentiation depending on the co-culture conditions with OB. In direct contact, EC enhance osteogenic differentiation, but in indirect cultures, EC suppress it. Our proteotranscriptomic analysis revealed that the osteosuppressive effect is related to the action of paracrine factors secreted by EC, while the osteoinductive properties of EC are mediated by the Notch signaling pathway, which can be activated only upon a physical contact of EC with OB. Indeed, in the direct co-culture, the knockdown of Notch1 and Notch3 receptors in EC has an inhibitory effect on the OB osteogenic differentiation, whereas activation of Notch by intracellular domain of either Notch1 or Notch3 in EC has an inductive effect on the OB osteogenic differentiation.

Conclusion The data indicate the dual role of the endothelium in regulating osteogenic differentiation and highlight the unique role of the Notch signaling pathway in inducing osteogenic differentiation during cell-to-cell interactions. The findings of the study emphasize the importance of intercellular communication in the regulation of osteoblast differentiation during bone development and maintenance.

*Correspondence:
Anna Malashicheva
malashicheva@incras.ru

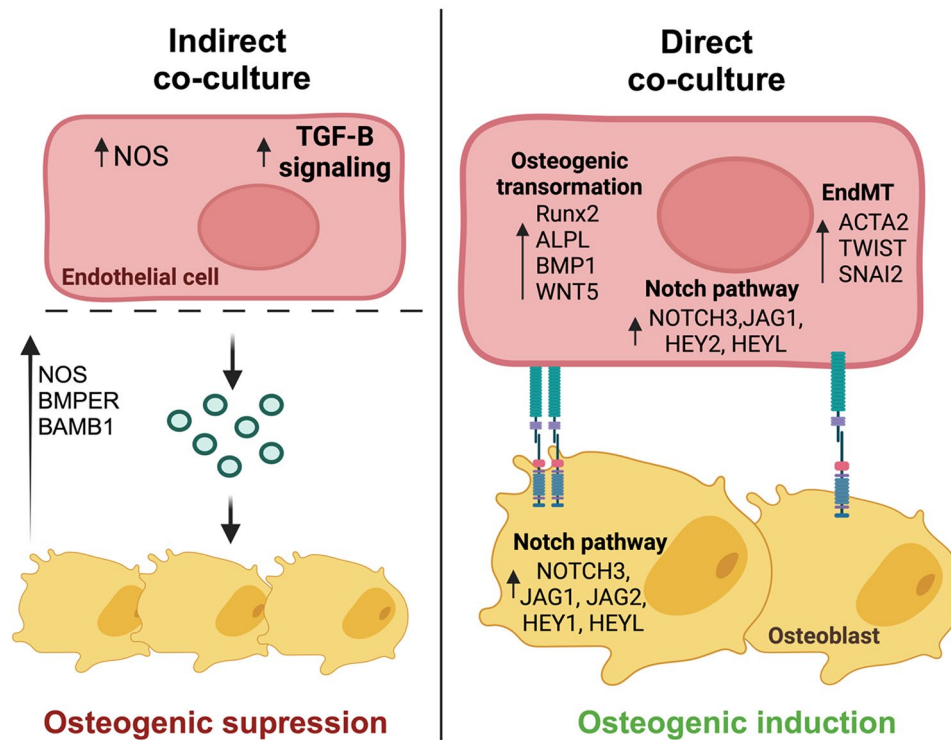
Full list of author information is available at the end of the article



© The Author(s) 2025, corrected publication 2025. **Open Access** This article is licensed under a Creative Commons Attribution-NonCommercial-NoDerivatives 4.0 International License, which permits any non-commercial use, sharing, distribution and reproduction in any medium or format, as long as you give appropriate credit to the original author(s) and the source, provide a link to the Creative Commons licence, and indicate if you modified the licensed material. You do not have permission under this licence to share adapted material derived from this article or parts of it. The images or other third party material in this article are included in the article's Creative Commons licence, unless indicated otherwise in a credit line to the material. If material is not included in the article's Creative Commons licence and your intended use is not permitted by statutory regulation or exceeds the permitted use, you will need to obtain permission directly from the copyright holder. To view a copy of this licence, visit <http://creativecommons.org/licenses/by-nc-nd/4.0/>.

Keywords Endothelial cells, Osteoblasts, Osteogenic differentiation, Notch signaling, Co-culture

Graphical Abstract



Introduction

The functional integrity of the bone system is based on the formation of new bone tissue, its remodeling and the maintenance of a bone-forming cell population: mesenchymal stem cells (MSC), osteoblasts (OB), and bone-resorbing cells— osteoclast [1]. Osteogenesis is largely controlled by the microenvironment created by the close proximity of blood vessels [2, 3]. Endothelial cells (EC) that line the inner surface of blood vessels provide oxygen and nutrient transport and contribute to the formation of a perivascular niche [4, 5]. EC can regulate adjacent cell mineralization and transform their own behavior in response to environmental changes [2, 6, 7].

It is generally believed that the main mechanism of interaction between EC and bone tissue cells is associated with paracrine signaling, which includes the secretion of proangiogenic and osteogenic factors that provide functional responses in both cell types [5]. During development and regeneration, bone-forming cells secrete various angiogenic factors that stimulate the growth of blood vessels [7–9]. MSC and OB, in turn, migrate to the vascularization area, and EC begin to secrete osteogenic factors— bone morphogenetic proteins (BMP) and extracellular matrix bone proteins, such as osteocalcin and

osteopontin, which promote bone cell differentiation and matrix calcification [10].

Thus, in bone tissue, EC promote the activation of specific signaling pathways, stimulating osteogenic cell differentiation through paracrine mechanisms [11–13]. On the contrary, the endothelium normally prevents calcification in the vascular system and disorders associated with EC functionality lead to abnormal changes in the microenvironment, decreased secretion of endothelial nitric oxide (NO) and increased secretion of osteogenic factors contributing to aberrant osteogenic differentiation and ectopic calcification [14, 15].

However, it seems that not only paracrine factors have a significant effect on calcification processes [16, 17], but it is also important to consider the role of juxtacrine signaling in the interaction between EC and cells that can undergo osteogenic differentiation. Juxtacrine signaling implies cell-cell interactions through various protein molecules located on the surface of cells. In the context of angio-osteogenesis it can be implemented in the following ways: through cell adhesion molecules— integrins and cadherins binding to extracellular matrix proteins (ECM) [18]; through gap junctions— connexins [19] and through ligand-receptor interactions, namely through the Notch signaling pathway [16, 20].

Uncovering the intricate mechanisms that govern the interaction between endothelial and osteogenic cells is crucial to understanding the balance between bone homeostasis in bone and abnormal mineralization processes in cardiovascular tissues. This study aimed to investigate paracrine and juxtacrine mechanisms that mediate crosstalk between EC and OB in the context of osteogenic cell differentiation *in vitro*. To distinguish these two types of interaction, we co-cultured OB and EC directly to activate juxtacrine signaling (direct co-culture) or separated them by a membrane penetrable to paracrine factors, but not to cells (indirect co-culture).

We demonstrate here that the presence or absence of direct contact between human osteoblasts and endothelial cells during the induction of osteogenic differentiation can lead to either osteoinductive or osteosuppressive effects. This novel finding underlies the crucial role of Notch signaling and physical interactions between osteoblasts and endothelial cells in osteogenic differentiation and provide a potential basis for the therapeutic management of osteogenic differentiation-related pathologies based on Notch signaling.

Materials and methods

Cell culture

Osteoblast isolation

Human osteoblast cell cultures (OB) were isolated from biopsies of the spongy bone tissue epiphysis of the femur or tibia obtained from patients during knee or hip replacement surgery. Bone material from the patients was provided by the Russian Scientific Research Institute of Traumatology and Orthopedics named after R.R.Vreden. The protocol of the clinical trial was approved by the local Ethics Committee of the National Medical Research Center for Traumatology and Orthopedics named after R.R.Vreden and corresponded to the principle of the Helsinki Declaration. All patients gave informed consent.

To isolate OB from the spongy bone tissue material, the samples were washed with a phosphate-salt buffer (PBS) (Biolot, Russia) with the addition of 1% penicillin/streptomycin solution (Gibco, USA), after that, using carbide pliers, the biopsies were divided into small fragments up to 0.5 mm in size.

The fragments were repeatedly washed with PBS and then the homogenized bone mass was placed in a 0.2% solution of type II collagenase (Worthington Biochemical Corporation, USA) and incubated for 30 min at 37 °C, after which they were washed with PBS and transferred to 0.2% collagenase IV (Worthington Biochemical Corporation, USA) and incubated for 16 h at 37 °C. After 16 h, bone fragments were washed with a growth nutrient medium with the addition of 15% fetal bovine serum (FBS) (Hy Clone, Cytiva, USA) to inactivate collagenase and were seeded on T75 flasks and cultivated for several

weeks in a DMEM nutrient medium (Gibco, USA) with an increased glucose content (4.5 g/l), the addition of 15% FBS, 1% solution of penicillin/streptomycin antibiotics (Gibco, USA), 2 mM glutamine (Gibco, USA) and 0.05 mM ascorbic acid solution (Sigma, USA) at 37 °C. The medium was changed every 3–4 days. The cells were cultivated up to the formation of a confluent monolayer. Then the cells were passaged and used for experiments for 2–5 passages. The cell population of primary osteoblasts used is homogeneous and was characterized in more detail in our previous publication [21].

Endothelial cell isolation

Human umbilical vein endothelial cells (HUVEC hereinafter EC) were acquired from the Pokrovsky Stem Cell Bank. The EC were cultivated at 37 °C in an ECM medium (ScienCell, USA) with the addition of growth factors, the 1% penicillin/streptomycin and 2 mM L-glutamine.

Continuous cell lines

The HEK293T cells were cultivated at 37 °C in the DMEM medium (Gibco, USA) with an increased glucose content (4.5 g/l) and the addition of 10% FBS, 1% penicillin/streptomycin and 2 mM L-glutamine.

Osteogenic differentiation

To induce osteogenic differentiation, we utilized a standard osteogenic medium typically employed for *in vitro* osteogenic differentiation: DMEM supplemented with 10% FBS, 2 mM L-glutamine, penicillin/streptomycin, 50 mg/ml ascorbic acid (Sigma, USA), 0.1 mM dexamethasone (Sigma, USA), and 10 mM β -glycerophosphate (Sigma, USA) [22]. The medium was changed every 3–4 days, supplemented with fresh osteogenic factors. Undifferentiated cells were used as controls for the experiments.

Direct co-culture of endothelial cells and osteoblasts

OB were seeded at the concentration of 200×10^3 and 60×10^3 cells per well on 6- and 24-well plates coated with 0.2% gelatin in the relevant nutrient medium. 24 h after OB adhered to the plastic, EC in concentrations of 200×10^3 and 60×10^3 , respectively, were sown on a monoculture of OB. After EC adhesion, the medium was replaced with the osteogenic medium. The medium was changed every 3–4 days, supplemented with fresh osteogenic factors.

Indirect co-culture of endothelial cells and osteoblasts

OB were seeded at a concentration of 200×10^3 and 60×10^3 cells per well on 6- and 24- well plates coated with 0.2% gelatin in the relevant nutrient medium. 24 h after the OB adhered to the plastic, transwell inserts

with a semipermeable membrane (Corning, USA) of the appropriate size were placed in the wells with the cells and were used in accordance with the manufacturer's instructions. EC were seeded in the transwell inserts at the concentrations of 200×10^3 and 60×10^3 , respectively. After adhesion of EC to a semipermeable membrane, osteogenic differentiation was induced in an indirect co-culture. The medium was changed every 3–4 days, supplemented with fresh osteogenic factors.

Alizarin red staining

Deposits of calcium phosphate minerals were detected by the alizarin red staining (Sigma, USA) after 21 days of cultivation. After cultivation, the cells were washed with PBS, then fixed in 70% ethanol, washed with distilled water and incubated in a solution of alizarin red for 20–30 min. The calcification intensity was quantified using a modified alizarin red extraction technique, where a 10% acetic acid solution was added, incubated for 10 min, and the color intensity was measured on a spectrophotometer (PICON, Russia) at 420 nm.

Lentiviral transduction

Lentiviral particles production

Lentiviral production was performed as described previously [23]. In brief, for the lentiviral particles production, HEK293T cells were seeded on 10 cm² Petri dishes in a concentration of 3.5 million cells in the appropriate nutrient medium. After 24 h, a transfecting mixture was added to the cells in a quantity of 10% of the volume of the nutrient medium consisting of 1 ml of OPTI MEM (Gibco, USA), 15 mg plasmid of interest, 9.73 mg packaging plasmid psPAX2 and 5.27 mg pMD2.G and 60 ml polyethylene adenimine (PEI) (Polysciences, USA). The plasmids of interest were plasmids, bearing short-hairpin RNA (shRNA) to the components of the Notch signaling pathway: shCSL, shNotch1-4, shDll4, shJag1, shRunx2, shMam1-3, cloned into the pLKO1-TRC cloning vector. The plasmids necessary for activation of the Notch signaling pathway were bearing the Notch intracellular domains 1, 3 (hNICD1, hNICD3), cloned into the pCIG3 vector. Lentiviral packaging plasmids were provided by D. Trono (Ecole Polytechnique Federale de Lausanne, Switzerland) and other plasmids were provided by A. Tomilin (the Laboratory of Molecular Biology of Stem Cells, INC RAS, Russia). After 18 h of transfection, the medium was replaced with a fresh one and cells were incubated for 24 h, then the nutrient medium was removed, transferred to a vial and centrifuged (5 min, 300 g). Then we filtered the medium and got an unconcentrated virus. To concentrate the virus, the nutrient medium was transferred into Polycarbonate centrifuge bottles (Beckman Coulter, USA) and centrifuged on an ultra-centrifuge (Beckman Coulter, Brea, USA) for 2 hours, 72,000 g.

After centrifuging, the supernatant was poured and 1% BSA solution (Sigma, USA) was added, the aliquoted and frozen at -80 °C before use. The virus titer was defined by a virus expressing GFP; transduction efficiency was estimated at 85–90%.

Lentiviral transduction of cells

A day before a cell cultures transduction with the lentiviral particles carrying the gene of interest, EC was seeded at the necessary concentration in 6- or 24- well tablets. EC were cultivated in the appropriate nutrient medium. After 24 h, the nutrient medium was removed and replaced with a transductive mixture: Opti-MEM medium, 1–10 µl of lentiviral particles and polybrene in the concentration of 5 mg/ml. Cells were cultivated in the presence of viral particles for 24 h, then the medium was removed and replaced with a fresh nutrient medium. 24 h after the medium change, cells were used in experiments: for co-cultivation with OB, for further isolation of total RNA and transcriptomic analysis.

OB co-cultivation with transduced endothelial cells

OB were seeded on 6- or 24-well plates coated with 0.2% gelatin at a concentration of 200×10^3 and 60×10^3 cells per well, respectively, in a nutrient medium. 24 h after the OB adhered to the plastic, the transduced EC were seeded on the OB monoculture at a concentration of 200×10^3 and 60×10^3 , respectively. Osteogenic differentiation was induced 24 h after EC adhesion to OB. The nutrient medium was changed every 3–4 days with the addition of fresh.

Magnetic sorting of CD31⁺/- cells

After 48 h of direct co-cultivation OB and EC were treated with 5% trypsin (Gibco, USA), the action of trypsin was inactivated with a nutrient medium with the addition of 15% FBS, the cell suspension was then resuspended and centrifuged. The co-culture separation was performed by the magnetic sorting using CD31⁺ endothelial marker using the MACS Cell Separation kit (Miltenyi Biotec, USA), according to the manufacturer's protocol. The resulting cell suspensions, the sediment of CD31⁻ (Osteoblasts) and CD31⁺ (Endothelial cells) cells were used for further isolation of total RNA and protein.

Gene expression analysis

Total RNA

The Total RNA was isolated with TriZol (Invitrogen, USA) by standard phenol/chloroform extraction procedure according to the manufacturer's instructions. Cells were washed with PBS and were lysed with the help of TriZol for 5 min at room temperature. Then lysates were transferred to microcentrifuge vials and mixed with 1/5 volume of chloroform. The samples were incubated

for 2 min and centrifuged (15 min, 12000 g, 4 °C). The aqueous phase was mixed with ½ of the original volume of TriZol ice isopropanol. After incubation, the samples were centrifuged for 10 min (12,000 g, 4 °C). The sediment was washed with 70% ethanol, air-dried at room temperature and dissolved in water. The quality of RNA was assessed by spectrometry Nanodrop (Thermo Fisher Scientific, USA) and electrophoresis in 1.5% agarose gel.

Real-time PCR

Total RNA (1 µg) was reverse transcribed with MMLV RT kit (Eurogen, Russia). Real-time PCR was performed with 1 µL cDNA and SYBRGreen PCR Mastermix (Eurogen, Russia) in the Light Cycler system (Roche, Switzerland) using specific forward and reverse primers for target genes. Corresponding gene expression level was normalized to either *HPRT* or *GAPDH*. Changes in target genes expression levels were calculated as fold differences using the comparative $\Delta\Delta CT$ method. Primer-BLAST software was used to develop target primers. All primer sequences will be presented at request. For the RT-qPCR analysis was performed with 5 biological replicate and 2 technical replicates.

Transcriptomic analysis

For transcriptomic analysis, total EC and OB RNA from 3 donors were used in three states: control samples (monocultures), samples after direct and indirect co-cultivation. 48 h after induction of osteogenic differentiation in co-cultures total RNA was isolated from cells. Total RNA in the amount of 500 ng for each sample was used to prepare RNA-sequencing libraries using the “CORALL Total RNA seq Library Prep Kit” with poly-A RNA selection in accordance with the manufacturer’s recommendations. The quality of the obtained libraries was verified by capillary electrophoresis on Agilent Bioanalyzer 2100 (Agilent Technologies). Finally, the libraries were sequenced on the Illumina NextSeq550 platform using one-sided reagents. All samples were sequenced simultaneously.

The quality control of the reads was carried out using the FASTQC and MultiQC. The reads were then compared to the reference genome of GRCh38 *Homo sapiens* using the STAR [24] with further quantification using the featureCounts [25]. Statistical data analysis was performed in R in the R Studio.

Co-cultivation of EC and OB. Statistical analysis of transcriptomic data

The DESeq2 library was used to analyze differential gene expression. The gene names were converted using the bitr function of the clusterProfile library [26], then the genes with a low count number were deleted. Next, the samples of rlog-normalized data were clustered by principal component analysis (PCA) and sparsity partial

least-squares discriminant analysis (sPLS-DA). The analysis of differential gene expression was carried out using the DESeq2 [27] library by a standard algorithm in accordance with pairs of direct-control, indirect-control and indirect-direct comparisons. The pathway enrichment analysis was carried out using the clusterProfile library. EnhancedVolcano and ggplot2 [28] libraries were used to visualize the results.

Transduced EC. Statistical analysis of transcriptomic data

Statistical analysis of RNA-sequencing data was performed using the DESeq2. The low-counted genes were deleted during the data filtration. HUVEC+shGFP samples were set as a control. When searching for differentially expressed genes, Wald significance tests with an adjusted p-value threshold <0.05 were used. The genes whose expression changed most significantly were selected according to $|\text{Log}_2\text{-Fold Change}| > 1$. Next, we performed rlog transformation of the data and clustered rlog-normalized data using principal component analysis (PCA). Based on the found differentially expressed genes, the pathway enrichment analysis was carried out using the KEGG database and the “Biological Processes” gene ontology using the clusterProfiler library. The analysis of DEG enrichment was carried out on the basis of the human genome annotation org.Hs.eg.db. Ggplot2, pheatmap and EnhancedVolcano were used to visualize the results of differential gene expression analysis.

Proteomic analysis

For proteomic analysis, protein from 4 donors were used in three states: control samples (monocultures), samples after direct and indirect co-cultivation. The protein was precipitated from the remaining organic phase of TRIzol after RNA isolation by 4 volumes of glacial acetone (LC-MS Grade) overnight at -20 °C. The precipitate was washed with methanol and dried in air, after which it was resuspended in 8 M urea (Sigma Aldrich, St. Louis, Missouri, USA) in 50 mM ammonium bicarbonate (Sigma Aldrich, St. Louis, Missouri, USA).

The protein concentration was then measured using a Qubit 4.0 (Thermo Fisher Sci, USA) using the QuDye Protein Quantification Kit (Lumiprobe, Moscow, Russia). 20 mcg of protein from each sample were incubated for an hour at 37 °C with 5 mM DTT (Sigma Aldrich, USA) and then incubated with a 15 mM iodoacetamide (Sigma Aldrich, USA) solution for 30 min at room temperature. The samples were then diluted with seven volumes of 50 mM ammonium bicarbonate and incubated for 16 h at 37 °C with trypsin of the proteomic class (Trypsin Gold, Promega, Madison, USA) in an a of 1:50. Tryptic peptides were desalted using solid-phase extraction with handmade C18 StageTips, following the protocol described by Rappsilber et al. [29]. The desalted peptides

were concentrated using a Labconco Centrивap centrifugal concentrator (Labconco, USA) and dissolved in water containing 0.1% formic acid for subsequent LC-MS/MS analysis.

Approximately 500 ng of tryptic peptides were used for HPLC-MS/MS analysis with ion mobility on a TimsToF Pro mass spectrometer with a nanoElute UHPLC chromatograph. HPLC-MS was performed in a two-column separation mode using an Acclaim™ PepMap™ trap cartridge (5 mm) (Thermo Fisher Scientific, Waltham, MA, USA) and a separating Aurora series column with nano-Zero technology (C18, 25 cm × 75 μm ID, 1.6 μm particle size) in gradient mode at a flow rate of 400 nL/min and a column temperature of 40 °C. Phase A was a 0.1% aqueous solution of formic acid, phase B was a 0.1% solution of formic acid in acetonitrile. The gradient ranged from 2 to 35% of phase B for 40 min, then up to 85% of phase B for 5 min, followed by washing of 85% of phase B for 10 min. The column was equilibrated with 4 column volumes before each sample. For electrospray ionization, a CaptiveSpray ion source with a capillary voltage of 1600 V, a nitrogen flow of 3 l/min and a source temperature of 180 °C was used. Mass spectrometry was performed in the automatic DDA PASEF mode with a 0.5 s cycle in positive polarity with fragmentation of ions with at least two charges in the *m/z* range from 100 to 1700 and the ion mobility range from 0.85 to 1.30 1/K0.

Statistical analysis of proteomic data

Protein identification was conducted against the human reference proteome (UP000005640, downloaded on June 27, 2022), including the most common contaminants. DDA-PASEF (data-dependent acquisition, parallel accumulation-serial fragmentation) data analysis and spectral library generation were performed using FragPipe (v. 18.0) following the standard LFQ-MBR protocol. The parameters included a parent and fragment ion mass tolerance of 10 ppm, a false discovery rate (FDR) of less than 1% for proteins and peptides, up to two missed cleavage sites, and trypsin specificity following the “Keil rule” (cleavage after K or R, except before P). Carbamidomethylation of cysteines was set as a fixed modification, while oxidation of methionine and N-terminal acetylation of proteins were considered variable modifications.

The missing values were imputed by the impseq method in the NAGuideR [30]. Logarithmic transformation and quantile normalization of the data were then performed, followed by differential expression analysis using the limma package. We also performed samples ordination using principal component analysis (PCA) and sparsity partial least-squares discriminant analysis (sPLS-DA) in the MixOmics [31]. The pathways and gene ontologies enrichment analysis were carried out similarly to transcriptomic data. The intersection of transcriptomic

and proteomic data was visualized using Venn diagrams (ggvenn package) between all detected genes and proteins and for each individual comparison group. ggplot2, pheatmap and EnhancedVolcano were used to visualize the results of differential gene expression analysis.

Data availability

The datasets used and/or analyzed during the current study are available from the corresponding author on reasonable request. Sequencing data have been deposited in the SRA NCBI database with BioProject identifier PRJNA895749. The mass spectrometry proteomics data have been deposited to the ProteomeXchange Consortium via the PRIDE [32] partner repository with the dataset identifier PXD037385.

Results

EC enhance or suppress osteogenic differentiation of osteoblasts depending on the presence of physical contact

To study the effect of intercellular interactions between EC and OB on osteogenic differentiation, we used direct and indirect co-culture models. In the direct co-culture, the cells were cultured in physical contact. In contrast, the indirect co-culture employed transwell inserts, which are permeable to proteins and small molecules but physically separate the cell populations, preventing direct contact. (Fig. 1A). OB and EC monocultures were used as controls. Both co-cultures and monocultures were grown in standard and osteogenic medium (OM).

Our results showed that indirect co-culture completely suppressed osteogenic differentiation, while direct contact increased matrix calcification compared to OB monoculture (Fig. 1B-C). At earlier stages, using RT-PCR, we observed similar osteogenic marker expression in OB under different co-culture conditions, except for *COL1A1* for OB direct (Fig. 1D).

Thus, we found that, depending on whether there is direct contact between cells, EC can have both osteoinductive and osteosuppressive effects on OB osteogenic differentiation.

OB have similar profiles when co-cultured with EC, while EC exhibit distinct changes in their profiles under different co-culture conditions with OB

Next, we analyzed the proteomic and transcriptomic profiles of OB and EC under different conditions of co-cultivation (Fig. 2A).

During the bioinformatic analysis of OB, 22,351 transcripts and 2,966 proteins were identified (Fig. 2B). For EC were identified 22,539 transcripts and 3,073 proteins (Fig. 2C). Corresponding transcripts were found for most of the identified proteins. Principal component analysis (PCA) indicated that OB forms mixed clusters under direct, indirect, and control conditions according to both

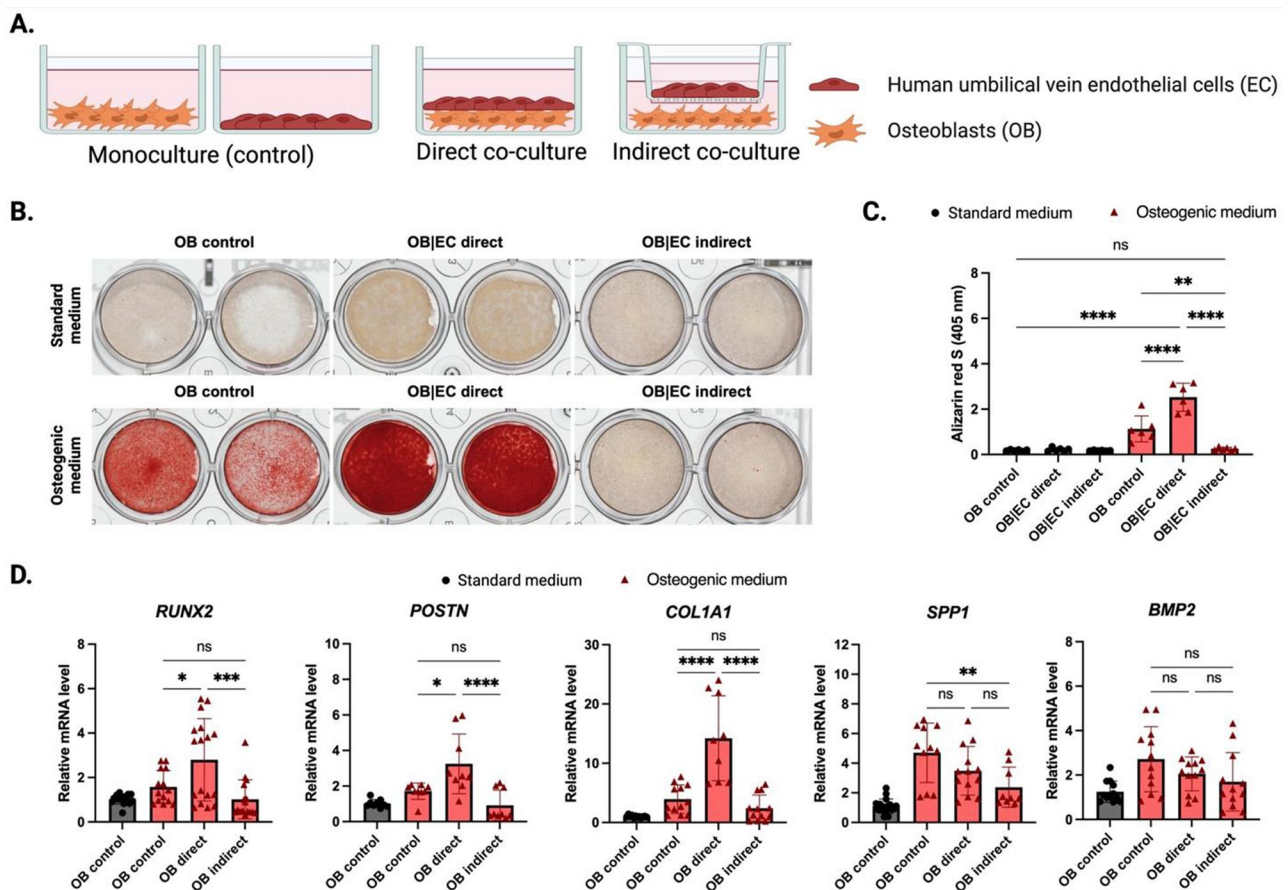


Fig. 1 The conditions of co-cultivation of EC and OB influence the osteogenic differentiation. **(A)** An experimental research model for a cultivation of EC and OB under contact and indirect conditions. **(B)** Representative images of the alizarin red staining under various cultivation conditions in standard and osteogenic media. **(C)** Quantitative assessment of the intensity of alizarin red staining by spectrophotometry. The results were analyzed using ANOVA, * $p < 0.05$, ** $p < 0.01$, and **** $p < 0.0001$. **(D)** The levels of expression of osteogenic markers *RUNX2*, *POSTN*, *COL1A1*, *SPP1*, *BMP2* in OB under various conditions after 48 h of co-cultivation with EC in the OM. OB were cultivated in standard and osteogenic media were used as a control. The relative mRNA levels of genes of interest are normalized according to *GAPDH* and presented as average values of expression level changes using the delta-delta Ct method. The results were analyzed using ANOVA, * $p < 0.05$, ** $p < 0.01$, **** $p < 0.0001$

transcriptomic and proteomic data (Fig. 2D). This suggest that when OB and EC are co-cultured, the OB profiles remain quite stable. Unlike osteoblasts EC displayed distinct proteomic and transcriptomic profiles under different conditions of co-cultivation with OB (Fig. 2E), indicating a significant endothelial response to various conditions of co-culture with OB.

For each cell type (OB and EC), we performed a differential analysis of transcript and protein expression in the following variations: OB direct vs. OB control (Supplementary Tables S1, S2), OB indirect vs. OB control (Supplementary Table S3), EC indirect vs. EC control (Supplementary Table S4, Supplementary Table S5) and EC direct vs. EC control (Supplementary Tables S6, S7).

When comparing OB direct with OB control, differential expression analysis demonstrated increased expression of osteogenic markers and Notch signaling pathway components (Fig. S1, Fig. S2). Gene Ontology (GO) analysis highlighted activated processes related to

extracellular matrix reorganization and cellular motility (Fig. S2C), while processes such as kinase activity, MAPK signaling, and cell proliferation were suppressed (Fig. S2D). Pathway analysis identified activation of cytokine-cytokine receptor and Notch signaling pathways, alongside suppression of Rap1 and Wnt signaling (Fig. S2F). Comparison of OB indirect to OB control found down-regulated transcripts (Supplementary Table S3, Fig. S3) associated with cell cycle (Fig. S3C), p53, and FoxO pathways (Fig. S3B).

Indirect co-cultivation with OB activates BMP inhibitors and nitric oxide synthase in EC

For EC indirect vs. EC control, 374 upregulated and 308 downregulated transcripts were identified, along with 42 upregulated and 17 downregulated proteins (Supplementary Tables S4, S5). Among upregulated elements, inhibitors of BMP signaling (e.g., *BMPER*, *MGP*, *BAMBI*), SMAD proteins (*SMAD6*, *SMAD7*, *SMAD9*),

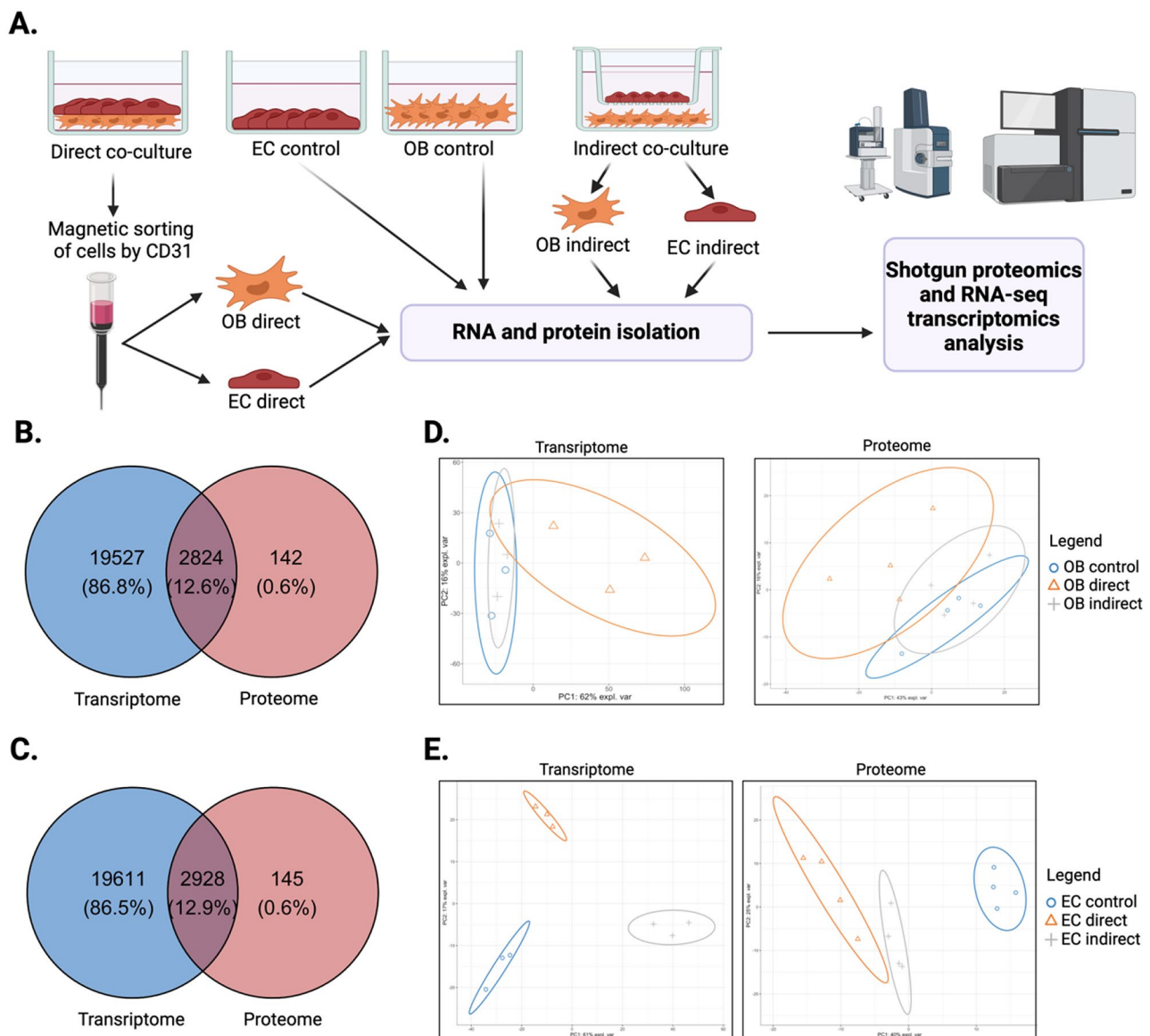


Fig. 2 Proteotranscriptomic analysis of OB and EC under different conditions of co-cultivation. **(A)** Schematic illustration of the experimental design to study the proteotranscriptomic profile of EC and OB under various conditions of co-cultivation. **(B–C)** Venn diagram showing the unique number of transcripts and proteins for OB **(B)** and EC **(C)**. **(D, E)** Principal component analysis (PCA) of transcriptomics and proteomics data showing the differences between OB **(D)** and EC **(E)** in various cultivation conditions. OB/EC control - standard cultivation in monoculture (control), OB/EC direct - direct co-cultivation with EC/OB followed separation using magnetic sorting by CD31, OB/EC indirect - separate co-cultivation with EC/OB on a semipermeable membrane

TGF- β ligands (e.g., *GDF3/Vgr-2*, *GDF5/BMP-14*, *GDF6/BMP-13*, *GDF7/BMP-12*) and *IHNBA* were prominent (Fig. 3A, Fig S7A). Jak/STAT pathway components were also significantly upregulated in both proteomic and transcriptomic data. *STAT1* displays a significant increase in its expression according to the transcriptomic data. Also, according to transcriptomic data, we detected an increase in expression of *STAT4* and *JAK3*. Finally, key factors important for the endothelium function, including nitric oxide synthase 1 (*NOS1*), *NOS3* and *KLF4*, exhibited increased expression.

GO analysis revealed activation of processes related to the circulatory system, BMP signaling, SMAD proteins, and extracellular matrix reorganization (Fig. 3C). Further analysis identified involvement of the TGF- β and cytokine-cytokine receptor interaction pathways (Fig. S6A), while downregulated transcripts were linked to cell adhesion (Fig. 3E) and Ras/PI3K-Akt signaling (Fig. S6B), which was also observed in proteomic data (Fig. S4).

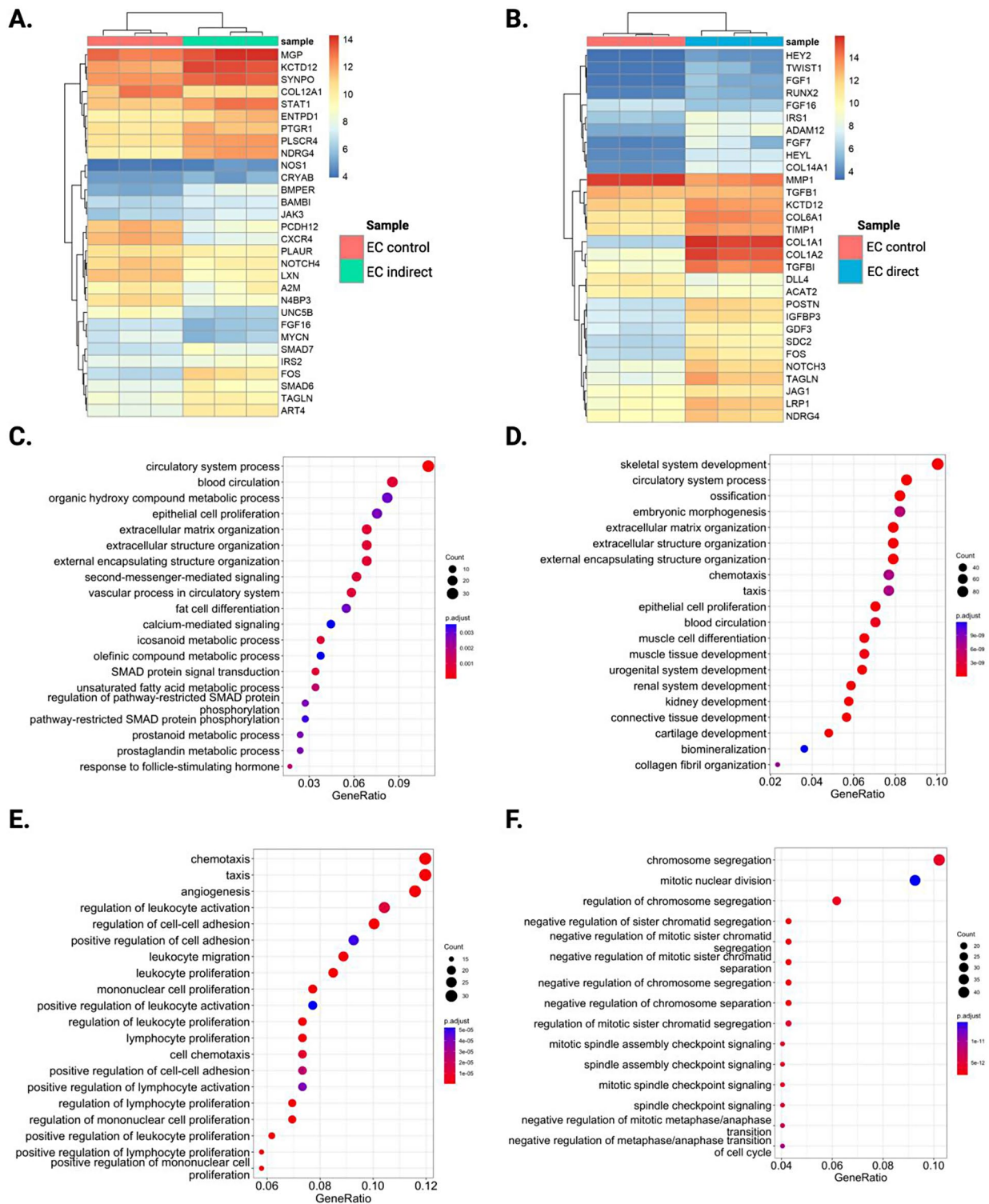


Fig. 3 Transcriptomic profile of EC in indirect/direct co-cultivation with OB. **(A, B)** Heatmap of differentially expressed genes (DEGs) by RNA seq in EC after indirect **(A)** and direct **(B)** co-cultivation with OB vs. EC control. **(C-F)** Enrichment analysis against «Biological processes» gene ontology of transcripts upregulated **(C)** and downregulated **(E)** in EC indirect and transcripts upregulated **(D)** and downregulated **(F)** in EC direct

The notch signaling pathway is activated when EC are co-cultured in contact with OB

For EC in direct co-culture, we identified 1,226 upregulated and 557 downregulated transcripts (Supplementary Table S6), along with 69 upregulated and 35 downregulated proteins (Supplementary Table S7).

As in the case of indirect co-cultivation, we have observed increased expression of components involved in BMP signaling (e.g., *BMP1*, *BMP8A*, *BMPRIA*, *GREM1*, *INHBA*, *MGP*, *GDF3*, *GDF5*, *FGF1*, *BMPER*, *SMAD6*, *SMAD7*, *SMAD9*) and Jak/STAT signaling (e.g., *JAK3*, *STAT2*, *STAT4*) (Fig. 3B, Fig S7B). Also, unlike EC indirect upregulation of the PI3K-Akt signaling pathway transcripts was observed in EC direct (Fig. S6C).

However, the overall direction of the response was entirely different - the most significant transcriptomic changes during direct co-cultivation were associated with skeletal development processes, involving key hub genes such as *RUNX2*, *ALPL*, *LOX*, *WNT5A*, *WNT5B*, and bone tissue collagens (*COL1A1*, *COL1A2*, *COL3A1*, *COL6A1*, *COL10A1*, *COL11A1*, *COL11A2*) (Fig. 3B, Fig S7B). Among the signaling pathways, the Notch pathway emerged as a major player. Notch components (*NOTCH3*, *DLL1*, *JAG1*) and their target genes (*HEY2*, *HEYL*) showed significant upregulation (Fig. 3B, Fig S7B). This pathway is known to promote endothelial-to-mesenchymal transition, consistent with the observed activation of *SNAI2*, *TWIST1* and *ACTA2* in direct co-cultivation. We have determined that only direct co-cultivation leads to increased expression levels of Notch signaling components, when OB and EC are cultured using the indirect cultivation method, there is no such increase observed in the expression of Notch receptors and ligands (Fig.S8).

GO analysis revealed that most of the upregulated transcripts (Fig. 3D, Fig. S6C) and proteins (Fig. S5B, D) were associated with biological processes such as ossification, focal adhesion, ECM reorganization, and ECM-receptor interaction. Conversely, the downregulated transcripts (Fig. 3F, Fig. S6D) were linked to chromosome segregation, cell cycle regulation, and potentially reduced EC proliferation.

Thus, our findings suggest that OB exhibit similar proteomic and transcriptomic profiles under different co-culture conditions with EC, while EC shown distinct molecular profiles, indicating their significant reaction to different conditions of co-cultured. We have found that indirect co-cultivation with OB stimulates the production of multiple inhibitors of the BMP signaling pathway in the EC, which is known to be a key driver of osteogenic differentiation. While, direct intercellular contact between EC and OB was found to activate the Notch signaling pathway. This Notch-mediated signaling, in turn,

induced the expression of genes associated with osteogenic differentiation within the EC population.

Osteogenic differentiation of OB can be regulated by modulation of notch signaling in EC during direct cell-cell contact

In order to find out how a decrease in the activity of various components of the Notch signaling pathway in EC affects the osteogenic differentiation of OB in direct co-culture, we transduced EC 48 h prior to co-cultivation with one of the lentiviral constructs carrying shRNA targeting the Notch pathway genes: *NOTCH1*, *NOTCH2*, *NOTCH3*, *NOTCH4*, *JAG1*, *DLL4*, *CSL*, *MAML1*, *MAML2*, and *MAML3* (Fig. 4A). The constructs were verified by qPCR (Fig.S9). As a control for lentiviral transduction, we used the shGFP vector, whose target gene is not expressed in cells, along with cells that underwent no viral transduction. Modified EC were cultivated with OB in the OM. After 14 days of co-cultivation, the co-culture was stained with alizarin red (Fig. 4B).

According to the staining results, it was revealed that a knockdown of some components of the Notch signaling pathway in EC (*NOTCH1*, *NOTCH3*, *NOTCH4* and *MAML1*) had an inhibitory effect on the osteogenic transformation of OB when co-cultured with modified EC in the OM. Moreover, the knockdown of *NOTCH1* and *NOTCH3* showed the strongest impact. In the next step, we investigated how the activation of Notch by the intracellular domain of either Notch1 or Notch3 in EC affects the osteogenic differentiation of OB during direct co-cultivation (Fig. 4C). Co-cultivation of OB with EC overexpressing the intracellular domain of Notch1 (NICD1) and Notch3 (NICD3) led to an increase in the level of calcification. Quantitative analysis of alizarin red staining intensity confirmed a statistically significant increase or decrease in the degree of osteogenic differentiation of OB relative to the control co-culture with EC transduced with shGFP (Fig. 4D).

The effect of notch activation/inactivation on the transcriptomic profile of EC

To elucidate which changes in EC resulting from inactivation/activation of the Notch signaling pathway influence osteogenic differentiation of OB, we identified transcriptomic profiles of EC modified with lentiviral constructs that activate NICD1 and NICD3 or inhibit *NOTCH1* and *NOTCH3* (Fig. 5A). These profiles were then compared to those of control EC transduced with shGFP.

During the analysis, 32,636 transcripts and their corresponding genes were identified. Differential expression gene (DEG) analysis showed that there were up to 1.5–1.7 times more DEGs detected in samples with activated intracellular Notch domains compared to those with inactivated Notch, respectively. This trend indicates that

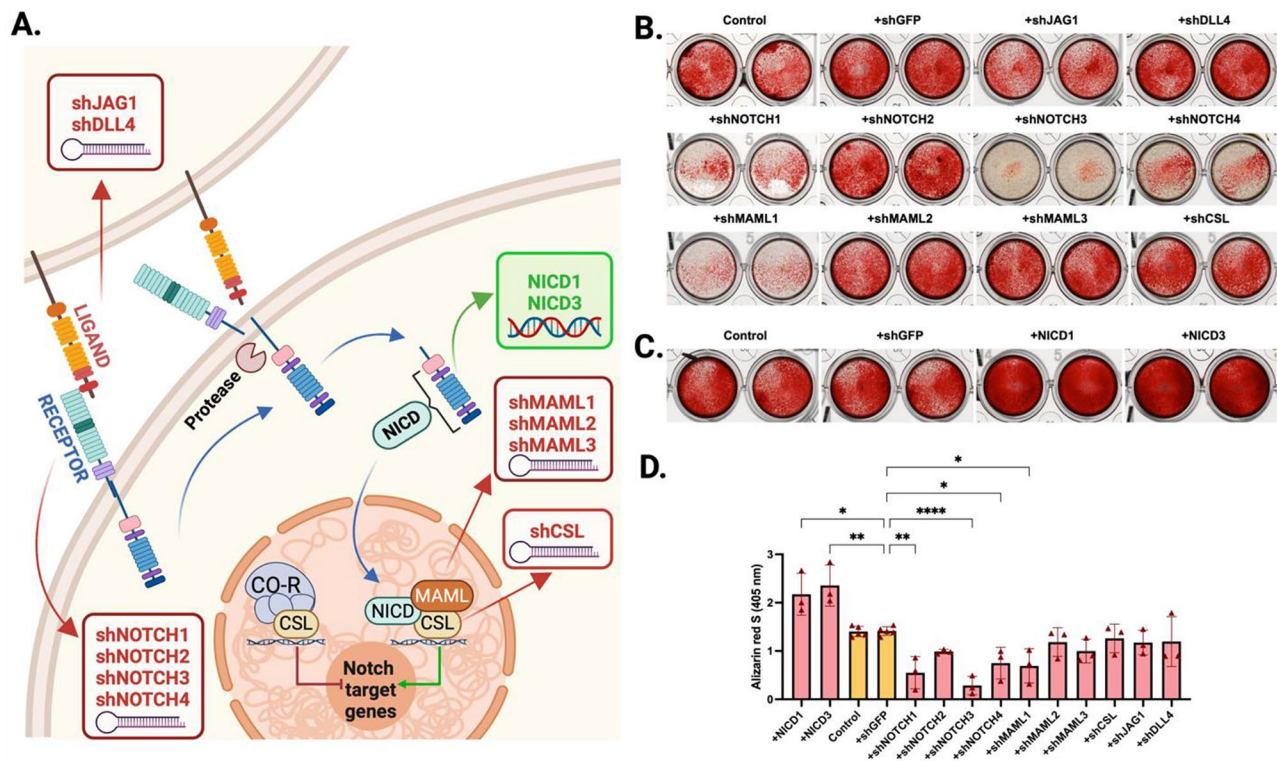


Fig. 4 Alizarin red staining of the direct co-culture of intact primary OB and transduced EC after 14 days of induced osteogenic differentiation. **(A)** Illustration of the Notch signaling pathway. The components of the Notch signaling pathway that were inhibited by lentiviral constructs are highlighted in red, while the activated components are shown in green. **(B–C)** The results of alizarin red staining after direct co-cultivation of OB with modified EC in the OM. The EC were previously modified 48 h prior to co-cultivation with OB using inhibitory **(B)** and activating **(C)** lentiviral constructs targeting components of the Notch signaling pathway. As a control of the lentiviral transduction, the shGFP vector was used, the target gene of which is not expressed in cells, as well as cells without viral load. **(D)** Quantitative assessment of the intensity of alizarin red staining by spectrophotometry. The results were analyzed using ANOVA, * $p < 0.05$, ** $p < 0.01$, **** $p < 0.001$ and compared them relative to the control co-culture there EC were transduced by shGFP, the target gene of which is not expressed in the EC (yellow column)

the activation of Notch intracellular domains contributes more to changes in the overall gene expression profile than a knockdown of Notch receptors. EC transduced by either shNOTCH1 or shNOTCH3 formed a mixed cluster while EC with overexpression of NICD1 and NICD3 also clustered close to each other on PCA but without overlapping (Fig. 5B). Further, we identified the top 10 differentially expressed genes that showed specific alterations in every group (Fig. 5C). EC with overexpression of NICD1 and NICD3 showed an increase in the expression of *ANGPTL2*, *PLVAP*, *LAMB3*, *SLCA4*, *MEST*, *SEMA5A*, *GUCY1A1*, *SLC46A3*, *SFRP1*, *SULF1*, *OFLML2A*, *ITGA11*, *LINC01614*, *COL8A* and *SDC2* compared to the shNOTCH1, shNOTCH3 and shGFP samples. For EC with knockdown of NOTCH1 and NOTCH3, the increased expression *DYSE*, *MMP10*, *PTGS1*, *SGK1*, *APLN*, *ANXA3*, *PLAT*, *MT2A*, *EDN1* and *CD247* genes was characteristic. We also found that both overexpression of NICD1 and NICD3 and knockdown of *NOTCH1* and *NOTCH3* in EC significantly reduced the expression of *ENSG00000284946*, *SPAG5*, *HMGB2*, *PLK1* and *PRC1*

compared to the control group of EC transduced with shRNA.

Additionally, we selected a set of genes that displayed a responsive transcriptional profile to the modulation of Notch signaling in both directions. We determined that in the EC with activated intracellular domains NICD1 and NICD3, the transcripts *GJA5*, *SULF1*, *SDC1*, *DLL4*, *TMT1*, *CRYAB*, *PTHLH* and *PCDH7* were upregulated. Conversely, in the EC transduced with shRNA targeting NOTCH1 and NOTCH3, the expression of these same transcripts was reduced compared to the control EC (Fig. 5D).

Functional annotation of DEGs, using Gene Ontology biological processes enrichment analysis, showed that DEGs that increased the expression level in EC with overexpression of NICD1 and NICD3 were linked to extracellular structures and extracellular matrix organization, as well as ossification in the case of NICD3 overexpression in EC (Fig. S10A, B). At the same time, metabolic pathways identified through the analysis were linked to TGF-beta signaling and the PI3K-AKT signaling pathway (Fig. S6A, B). For the knockout of NOTCH1 and NOTCH3 in

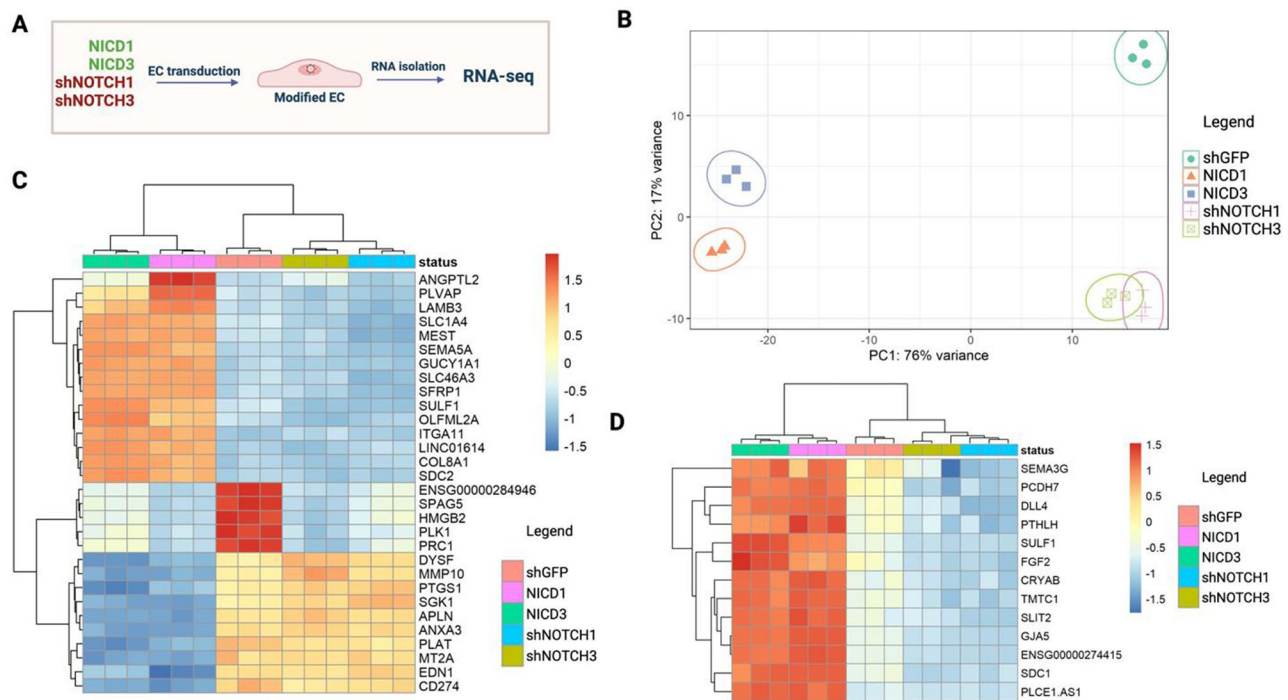


Fig. 5 Transcriptomic profile of EC during activation/inactivation of Notch. **(A)** Schematic illustration of the experimental design to study the transcriptomic profile of EC during activation/inactivation of Notch. **(B)** Principal component analysis (PCA), showing the multidimensional differences between EC overexpressing the intracellular domain of NICD1 and NICD3, and EC with inactivated *NOTCH1* and *NOTCH3* relative to control EC transduced by shGFP. **(C)** The heatmap of the top differentially expressed gene (DEGs) by RNA seq in EC. The control is EC, transduced by shGFP, the target gene of which is not expressed in EC. **(D)** The heatmap of the DEGs whose expression increased in the EC group with activated intracellular domains NICD1 and NICD3, and decreased in the EC group transduced with shRNA targeting *NOTCH1* and *NOTCH3*

EC, we observed downregulation of processes associated with chromosome segregation, DNA replication and the cell cycle (Fig. S10C, D).

Discussion

The crosstalk between the endothelium and bone-forming cells is a significant part of bone tissue formation. The microenvironment created by the endothelium is essential for successful bone regeneration [33], and the endothelial cell matrix facilitates osseointegration and mineralization [34]. In turn, osteogenic cells secrete paracrine factors and stimulate angiogenesis [35, 36]. The relationship between EC and bone-forming cells is a complex interaction based on both paracrine and juxtacrine signaling. Despite the numerous studies on the crosstalk of angio- and osteogenesis [5, 17, 37–42], many mechanisms of direct and indirect regulation remain insufficiently studied.

We demonstrate that EC in direct contact with OB enhance osteogenic differentiation, whereas the separation of these two cell types by a semipermeable membrane suppresses OB differentiation in vitro. Our data are consistent with previous conclusions indicating that direct contact with the endothelium is necessary for inducing osteogenic differentiation [17, 43] and that it

requires not only diffuse factors but also cell membrane proteins [44]. Interestingly, OB cultivated under different conditions showed similar expression of osteogenic markers and formed mixed clusters, as evidenced by the results of proteomic and transcriptomic analyses. Minor changes in the osteoblasts' proteomic profile during osteogenic differentiation induction were also evidenced by other studies [39], including our own [45, 46]. This suggests that it is the changes in EC, and not in OB, that are the main driver behind the observed suppression or enhancement of osteogenic differentiation.

In 2016, Shoham et al. made an important discovery and showed that in the developing bone tissue of a mouse embryo, the blood vessels within the bone lack a basal membrane [47]. Instead, the blood vessels are lined with type I collagen, which functions as the primary component of the ECM forming osteoid [47]. Additionally, their study demonstrated that EC can act as a template for mineral deposition, thereby mediating the process of bone formation. Notably, it was demonstrated that vasculature in bone itself can also mineralize [47]. Our data on the expression of components associated with skeletal development, such as RUNX2, ALPL, LOX, and various collagens (COL1A1, COL1A2, COL3A1, COL6A1, COL10A1, COL11A1, and COL11A2) in the

endothelium in direct contact with osteoblasts confirms Shoham et al.'s [47] conclusion that changes in vascular patterns play a crucial role in regulating bone morphogenesis, directing the formation of the collagen matrix and the subsequent mineral deposition.

In addition to the expression of osteogenic markers in EC during the contact co-cultivation, we observed an increase in TGF- β signaling components, one of the inducers of the endothelial-to-mesenchymal transition (EndMT) [48, 49]. It is known that EC can undergo the EndMT and eventually lose their characteristic endothelial markers while expressing mesenchymal markers instead, which is a critical process in various physiological and pathological conditions [50]. Initially, we hypothesized that the EndMT in the EC mediated by TGF- β signaling is one of the core mechanisms contributing to enhanced osteogenic differentiation. However, during bioinformatic analysis, a noteworthy observation was made: we found the activation of the TGF- β signaling pathway in the EC during both contact and indirect co-cultivation with OB. Nevertheless, the induction of osteogenic differentiation was only observed under conditions of direct co-cultivation. This suggests another critical factor or mechanism affecting the enhancement of osteogenic differentiation during the crosstalk between EC and OB.

Our results show that the Notch signaling pathway becomes activated during the interaction between EC and OB via direct physical contact. This signaling cascade appears to be a crucial regulator that initiates and guides the osteogenic differentiation program within the cells.

The Notch signaling pathway has a complex and diverse role in regulating bone biology, depending on various factors [51–54]. On the one hand, it supports the proliferation of MSCs and activates the differentiation of osteoblasts into osteocytes [55]. On the other hand, inhibition of Notch has been shown to promote osteoblast proliferation while suppressing their further differentiation [56]. Moreover, the interaction between EC and OB in the bone microenvironment makes an important contribution to regulating osteogenic differentiation via the Notch signaling pathway. Induced changes in normal blood flow in mice lead to decreased EC activity and subsequent decreases in bone formation correlated with a decrease in Notch signaling [57]. At the same time, reactivation of the Notch pathway in the EC restored local angiogenesis and stimulated bone tissue formation [57].

It is well known that the Notch signaling pathway plays a special role in abnormal osteogenic differentiation, which is a key factor in ectopic calcification [58, 59]. Therefore, we assumed that modulation of the Notch signaling pathway via EC may represent a promising therapeutic strategy aimed at both enhancing osteogenic differentiation of osteoblasts to repair damaged bone

tissue and suppressing pathological calcification processes. Our group has already demonstrated that Notch activation leads to osteogenic differentiation of aortic smooth muscle cells and that EC may trigger calcification mechanisms [60].

Based on the obtained results and literature data, we performed a series of experiments in which we transduced EC with various lentiviral constructs targeting genes associated with the Notch signaling pathway and studied their effect on osteogenic differentiation of osteoblasts in co-cultures. We found that knockdown of Notch1 and Notch3 receptors in EC suppressed osteogenic differentiation of OB, while activation of NICD1 and NICD3 stimulated it.

Our results are consistent with those of Lin et al., who reported an association between *ANGPTL2* and Notch activation [61]. Furthermore, it is already known that Notch signaling is associated with *PLVAP*, encoding the synthesis of an EC-specific protein [62]. Moreover, the *GUCY1A1* gene, which we identified, is a well-known Notch signaling effector in EC [63]. Another gene, *SFRP1*, has been shown to be regulated by *HEY/HES*, which in turn are targets of the Notch signaling [64]. *SULF1* participates in the differentiation of EC into arterial and venous cells and the suppression of its expression leads to a decrease in the expression of *NOTCH3*, one of the arterial markers [65]. Finally, the expression level of *SDC2* has been found to be closely related to the activity of Notch1 and Notch3, irrespective of the endothelial nature of the cells [66].

We also found several transcripts of *GJA5*, *SULF1*, *SDC1*, *DLL4*, *TMTC1*, *CRYAB*, *PTHLH*, *PCDH7*, *SEMA3G* and *FGF2* whose expression increased in the endothelial cell group with activated intracellular domains NICD1 and NICD3, and decreased in the EC group of transduced with shRNA targeting *NOTCH1* and *NOTCH3*. Previous studies have shown that *SULF1* can modulate the BMP signaling pathways [67], and *CRYAB* is a transcriptional target of the BMP pathway [68]. *CRYAB* is also an important regulator of osteogenic differentiation in cells of mesenchymal origin [69, 70], just like *FGF2* [71–73]. The gene *PTHLH*, which encodes parathyroid hormone-like hormone, has a complex regulatory role. It can not only contribute to the osteogenic differentiation of stem cells [74], but also affect the osteogenic transformation of vascular interstitial cells [75], promote dysfunction in valve endothelial cells, and participate in vascular calcification [75, 76]. In the work by Huang et al., it was shown that Notch1 activation in EC leads to the expression of *Sema3G* and can contribute to revascularization [77].

Additionally, the analysis of the identified DEGs along the KEGG pathways for modified EC showed that the TGF- β signaling pathway is activated under

the overexpression of NICD1 and NICD3. It suggests a strong interplay between the TGF- β and Notch signaling cascades, both of which are well-known critical regulators of osteogenic differentiation. Several studies underscore the importance of the interaction between TGF- β and Notch in the context of osteogenic differentiation. For example, in the study by Wagley et al., it was demonstrated that the Notch signaling pathway serves as a driver for osteogenic differentiation of osteoblasts mediated by BMP, the TGF- β signaling pathway components [78]. In the study by Cao et al., it was revealed that inhibition/activation of the Notch signaling pathway leads to either suppression or activation of BMP9-induced MSC osteogenic differentiation both in vitro and in vivo [79]. It is likely that the complex activation of these two pivotal signaling networks, Notch and TGF-beta, results in the expression of components necessary for the mineralization process, particularly collagens, in EC. The interplay between these two key signaling networks orchestrates the transition of EC towards a more osteogenic phenotype, enabling them to participate in mineralization and the activation of bone formation carried out by osteoblasts.

We also studied the phenomenon of osteogenic differentiation suppression during indirect co-cultivation of EC and OB. We found that EC stimulated the production of various inhibitors of the BMP signaling pathway. It is significant because the BMP signaling pathway has been believed to be one of the main factors for osteogenic differentiation [80, 81]. It has been previously shown that the BMP inhibitors discovered during this study BAMBI [82], SMAD6 [83], SMAD7 [84] inhibit osteogenic differentiation through a negative feedback mechanism. Interestingly, the literature indicates that certain BMP inhibitors, such as BMPER [85] and MGP [86], can function as positive regulators of osteogenic differentiation. Nevertheless, in the studies by Xiao and Zhang [85, 86], the regulation of these BMP inhibitors was carried out by modulation of their expression in osteogenic cells. In contrast to Xiao and Zhang's research, our study demonstrates the expression of BMP inhibitors by endothelial cells. This suggests that the source of these inhibitors may influence the final effect on bone mineralization. EC enhanced the production of multiple components involved in the Jak/STAT signaling cascade. Specifically, we observed an elevated expression of STAT1, which is known to interact with RUNX2, the master regulator of osteoblast differentiation [87]. This interaction has an inhibitory effect on the osteogenic differentiation of both osteoblasts [88] and mesenchymal stem cells of the bone marrow [89]. As a result, this STAT1-mediated suppression of RUNX2 activity ultimately impairs bone formation and regeneration processes [90]. We also observed that, in addition to BMP inhibitors and components of

Jak/STAT signaling pathway, indirect co-cultivation of EC and OB resulted in a notable increase in the expression of nitric oxide synthase (NOS1 and NOS3) enzymes, which affect the production of NO. Nitric oxide is known to play an important role in the crosstalk between endothelium and bone and controls key stages of angiogenesis and osteogenesis [91–93]. The study by Veeriah et al. has demonstrated that an increase in NO levels can enhance proliferation while suppressing osteoblast differentiation [94]. This is consistent with our own findings, which showed that during indirect co-cultivation, processes related to the cell cycle were activated in OB, but osteogenic differentiation did not occur. The role of endothelial NO has also been highlighted in a pathological calcification model, where endothelial NO from VEC was shown to prevent calcification of porcine VIC [59, 95]. This illustrates the delicate balance maintained by nitric oxide in regulating these crucial cellular processes at the interface of the endothelium and osteogenic differentiation.

Our research has revealed the pivotal significance of physical interactions between human endothelial cells and osteoblasts in the process of osteogenic differentiation, as well as the crucial role of the Notch signaling pathway in cell communication and the initiation of osteogenic signals. The findings presented in this study are of utmost importance for understanding the regulatory mechanisms of osteogenesis. They also have great significance for bioengineering and developing future therapeutic approaches to enhancing bone regeneration.

Conclusion

We found that endothelial cells have a dual effect on osteogenic differentiation processes. Osteosuppressive properties are associated with the action of paracrine factors secreted by endothelial cells. While the osteoinductive properties of endothelial cells are mediated by the Notch signaling pathway and are realized only in the presence of physical contact with mesenchymal cells. We determined that inactivation of Notch1 and Notch3 in endothelial cells suppresses osteogenic differentiation of osteoblasts, whereas active intracellular domains of Notch1 and Notch3 in endothelial cells activate osteogenic differentiation of endothelial-osteoblast co-cultures. Thus, modification of the Notch pathway of endothelial cells could be a tool for enhancing/inhibiting osteogenic differentiation of osteoblasts.

Abbreviations

MSC	Mesenchymal stem cells
OB	Osteoblasts
EC	Endothelial cells
SMC	Vascular smooth muscle cells
VC	Vascular calcification
VIC	Valve interstitial cells
CAVD	Calcific aortic valve disease
BMP	Bone morphogenetic proteins

NO	Nitric oxide
VEC	Aortic valve endothelial cells
ECM	Extracellular matrix
OM	Osteogenic medium
DEG	Differential expressed genes
NOS	Nitric oxide synthase
PBS	Phosphate buffered saline

Supplementary Information

The online version contains supplementary material available at <https://doi.org/10.1186/s12964-025-02096-0>.

Supplementary Material 1
Supplementary Material 2
Supplementary Material 3
Supplementary Material 4
Supplementary Material 5
Supplementary Material 6
Supplementary Material 7
Supplementary Material 8

Acknowledgements

We thank A. Kostina and A. Kiselev for the technical assistance with designed and synthesized plasmids. We thank Core Facility "Centre for Molecular and Cell Technologies" (St. Petersburg State University).

Author contributions

Conceptualization, A.M.; methodology, D.P.; investigation, D.P., L.B., K.A., N.A.; collection and/or assembly of data, data analysis and interpretation P.K., A.L., I.K., resources, V.U., S.B.; writing—original draft preparation, D.P., A.M.; writing—review and editing, A.M., D.P., visualization, D.P.; supervision, A.M.; funding acquisition, A.M.

Funding

This work was supported by a grant from the Russian Science Foundation 23-15-00320 "Mechanisms of regulation of osteogenic differentiation in normal conditions and in cardiovascular pathology" (to Anna Malashicheva).

Data availability

Proteomic data are available through ProteomeXchange under the identifier PXD037385. Transcriptomic data have been deposited in the NCBI SRA database under the BioProject Identifier PRJNA895749.

Declarations

Ethics approval and consent to participate

This study was approved by the local Ethical Committee of Vreden National Medical Research Center of Traumatology and Orthopedics, Saint-Petersburg, Russia.

Consent for publication

All authors have read and agreed to the published version of the manuscript.

Competing interests

The authors declare no competing interests.

Author details

¹Institute of Cytology RAS, Saint-Petersburg, Russia

²Vreden National Medical Research Center of Traumatology and Orthopedics, Saint-Petersburg, Russia

Received: 28 November 2024 / Accepted: 8 February 2025

Published online: 19 February 2025

References

1. Stegen S, Carmeliet G. Metabolic regulation of skeletal cell fate and function. *Nat Rev Endocrinol*. 2024;20:399–413.
2. Grosso A, Burger MG, Lunger A, Schaefer DJ, Banfi A, Di Maggio N. It takes two to Tango: Coupling of Angiogenesis and Osteogenesis for Bone Regeneration. *Front Bioeng Biotechnol*. 2017;5.
3. Sivan U, De Angelis J, Kusumbe AP. Role of angiocrine signals in bone development, homeostasis and disease. *Open Biol*. 2019;9:190144.
4. Matta R, Feng Y, Sansing LH, Gonzalez AL. Endothelial cell secreted VEGF-C enhances NSC VEGFR3 expression and promotes NSC survival. *Stem Cell Res*. 2021;53:102318.
5. Stegen S, Carmeliet G. The skeletal vascular system—breathing life into bone tissue. *Bone*. 2018;115:50–8.
6. Howe KL, Fish JE. Transforming endothelial cells in atherosclerosis. *Nat Metab*. 2019;1:856–7.
7. Augustin HG, Koh GY. Organotypic vasculature: From descriptive heterogeneity to functional pathophysiology. *Science* (1979). 2017;357.
8. Duan X, Murata Y, Liu Y, Nicolae C, Olsen BR, Berendsen AD. Vegfa regulates perichondrial vascularity and osteoblast differentiation in bone development. *Development*. 2015;142:1984–91.
9. Xu R, Yallowitz A, Qin A, Wu Z, Shin DY, Kim J-M, et al. Targeting skeletal endothelium to ameliorate bone loss. *Nat Med*. 2018;24:823–33.
10. Hu DP, Ferro F, Yang F, Taylor AJ, Chang W, Miclau T, et al. Cartilage to bone transformation during fracture healing is coordinated by the invading vasculature and induction of the core pluripotency genes. *Development*. 2017;144:221–34.
11. Yallowitz AR, Shim J-H, Xu R, Greenblatt MB. An angiogenic approach to osteoanabolic therapy targeting the SHN3-SLIT3 pathway. *Bone*. 2023;172:116761.
12. Huang J, Han Q, Cai M, Zhu J, Li L, Yu L, et al. Effect of angiogenesis in bone tissue Engineering. *Ann Biomed Eng*. 2022;50:898–913.
13. Stucker S, Chen J, Watt FE, Kusumbe AP. Bone angiogenesis and vascular niche remodeling in stress, aging, and diseases. *Front Cell Dev Biol*. 2020;8.
14. Kraller S, Blaser MC, Aikawa E, Camici GG, Lüscher TF. Calcific aortic valve disease: from molecular and cellular mechanisms to medical therapy. *Eur Heart J*. 2022;43:683–97.
15. Driscoll K, Cruz AD, Butcher JT. Inflammatory and Biomechanical Drivers of Endothelial-Interstitial Interactions in calcific aortic valve disease. *Circ Res*. 2021;128:1344–70.
16. Ramasamy SK, Kusumbe AP, Wang L, Adams RH. Endothelial notch activity promotes angiogenesis and osteogenesis in bone. *Nature*. 2014;507:376–80.
17. Cao C, Huang Y, Tang Q, Zhang C, Shi L, Zhao J, et al. Bidirectional juxtacrine ephrinB2/Ephs signaling promotes angiogenesis of ECs and maintains self-renewal of MSCs. *Biomaterials*. 2018;172:1–13.
18. Menge T, Gerber M, Wataha K, Reid W, Guha S, Cox CS, et al. Human mesenchymal stem cells inhibit endothelial proliferation and angiogenesis via cell–cell contact through modulation of the VE-Cadherin/ β -Catenin signaling pathway. *Stem Cells Dev*. 2013;22:148–57.
19. Liao Y, Fang Y, Zhu H, Huang Y, Zou G, Dai B et al. Concentrated growth factors promote hBMSCs osteogenic differentiation in a Co-culture System with HUVECs. *Front Bioeng Biotechnol*. 2022;10.
20. Liu W, Zou M, Chen M, Zhang Z, Mao Y, Yang Y, et al. Hypoxic environment promotes angiogenesis and bone bridge formation by activating Notch/RBPJ signaling pathway in HUVECs. *Genomics*. 2024;116:110838.
21. Kostina D, Lobov A, Klausen P, Karelkin V, Tikhilov R, Bozhkova S, et al. Isolation of human osteoblast cells capable for mineralization and synthesizing bone-related proteins in Vitro from Adult Bone. *Cells*. 2022;11:3356.
22. Lobov A, Malashicheva A. Osteogenic differentiation: a universal cell program of heterogeneous mesenchymal cells or a similar extracellular matrix mineralizing phenotype? *Biol Commun*. 2022;67.
23. Malashicheva A, Kanzler B, Tolkunova E, Trono D, Tomilin A. Lentivirus as a tool for lineage-specific gene manipulations. *Genesis*. 2007;45:456–9.
24. Dobin A, Davis CA, Schlesinger F, Drenkow J, Zaleski C, Jha S, et al. STAR: ultrafast universal RNA-seq aligner. *Bioinformatics*. 2013;29:15–21.
25. Liao Y, Smyth GK, Shi W. featureCounts: an efficient general purpose program for assigning sequence reads to genomic features. *Bioinformatics*. 2014;30:923–30.
26. Yu G, Wang L-G, Han Y, He Q-Y. clusterProfiler: an R Package for comparing Biological themes among Gene clusters. *OMICS*. 2012;16:284–7.
27. Love MI, Huber W, Anders S. Moderated estimation of Fold change and dispersion for RNA-seq data with DESeq2. *Genome Biol*. 2014;15:550.
28. Wickham H. ggplot2. Cham: Springer International Publishing; 2016.

29. Rappsilber J, Mann M, Ishihama Y. Protocol for micro-purification, enrichment, pre-fractionation and storage of peptides for proteomics using StageTips. *Nat Protoc.* 2007;2:1896–906.
30. Wang S, Li W, Hu L, Cheng J, Yang H, Liu Y. NAGuideR: performing and prioritizing missing value imputations for consistent bottom-up proteomic analyses. *Nucleic Acids Res.* 2020;48:e83–83.
31. Rohart F, Gautier B, Singh A, Lê Cao K-A, mixOmics. An R package for 'omics feature selection and multiple data integration. *PLoS Comput Biol.* 2017;13:e1005752.
32. Perez-Riverol Y, Bai J, Bandla C, García-Seisdedos D, Hewapathirana S, Kamatchinathan S, et al. The PRIDE database resources in 2022: a hub for mass spectrometry-based proteomics evidences. *Nucleic Acids Res.* 2022;50:D543–52.
33. Chen W, Xu K, Tao B, Dai L, Yu Y, Mu C, et al. Multilayered coating of titanium implants promotes coupled osteogenesis and angiogenesis in vitro and in vivo. *Acta Biomater.* 2018;74:489–504.
34. He Y, Wang W, Lin S, Yang Y, Song L, Jing Y, et al. Fabrication of a bio-instructive scaffold conferred with a favorable microenvironment allowing for superior implant osseointegration and accelerated in situ vascularized bone regeneration via type H vessel formation. *Bioact Mater.* 2022;9:491–507.
35. Rao RR, Peterson AW, Ceccarelli J, Putnam AJ, Stegemann JP. Matrix composition regulates three-dimensional network formation by endothelial cells and mesenchymal stem cells in collagen/fibrin materials. *Angiogenesis.* 2012;15:253–64.
36. Zhang L, Qian Z, Tahtinen M, Qi S, Zhao F. Prevascularization of natural nanofibrous extracellular matrix for engineering completely biological three-dimensional prevascularized tissues for diverse applications. *J Tissue Eng Regen Med.* 2018;12.
37. Lin X, Shan S-K, Xu F, Zhong J-Y, Wu F, Duan J-Y, et al. The crosstalk between endothelial cells and vascular smooth muscle cells aggravates high phosphorus-induced arterial calcification. *Cell Death Dis.* 2022;13:650.
38. Tuckermann J, Adams RH. The endothelium–bone axis in development, homeostasis and bone and joint disease. *Nat Rev Rheumatol.* 2021;17:608–20.
39. Simunovic F, Steiner D, Pfeifer D, Stark GB, Finkenzeller G, Lampert F. Increased extracellular matrix and proangiogenic factor transcription in endothelial cells after cocultivation with primary human osteoblasts. *J Cell Biochem.* 2013;114:1584–94.
40. Kocheva I, Bryja A, Mozdzik P, Volponi AA, Dyszkiewicz-Konwińska M, Piotrowska-Kempisty H et al. Human umbilical vein endothelial cells (HUVECs) co-culture with osteogenic cells: from molecular communication to engineering prevascularized bone grafts. *J Clin Med.* 2019;8.
41. Bixel MG, Sivaraj KK, Timmen M, Mohanakrishnan V, Aravamudan A, Adams S, et al. Angiogenesis is uncoupled from osteogenesis during calvarial bone regeneration. *Nat Commun.* 2024;15:4575.
42. Novak S, Tanigawa H, Singh V, Root SH, Schmidt TA, Hankenson KD et al. Endothelial to mesenchymal notch signaling regulates skeletal repair. *JCI Insight.* 2024;9.
43. Villars F, Guillotin B, Amédée T, Dutoya S, Bordenave L, Bareille R, et al. Effect of HUVEC on human osteoprogenitor cell differentiation needs heterotypic gap junction communication. *Am J Physiol-Cell Physiol.* 2002;282:C775–85.
44. Villars F, Bordenave L, Bareille R, Amédée J. Effect of human endothelial cells on human bone marrow stromal cell phenotype: role of VEGF? *J Cell Biochem.* 2000;79:672–85.
45. Khvorova IA, Kostina DA, Zainullina BR, Fefilova EA, Gromova ES, Tikhilov RM, et al. Osteogenic differentiation in Vitro of human osteoblasts is Associated with only slight shift in their proteomics Profile. *Cell Tissue Biol.* 2022;16:540–6.
46. Lobov A, Kuchur P, Khizhina A, Kotova A, Ivashkin A, Kostina D, et al. Mesenchymal cells retain the specificity of Embryonal Origin during osteogenic differentiation. *Stem Cells.* 2024;42:76–89.
47. Ben Shoham A, Rot C, Stern T, Krief S, Akiva A, Dadosh T et al. Deposition of collagen type I onto skeletal endothelium reveals a new role for blood vessels in regulating bone morphology. *Development.* 2016.
48. Piera-Velazquez S, Jimenez SA. Endothelial to mesenchymal transition: role in physiology and in the Pathogenesis of Human diseases. *Physiol Rev.* 2019;99:1281–324.
49. Fan L, Yao D, Fan Z, Zhang T, Shen Q, Tong F, et al. Beyond VICs: shedding light on the overlooked VECs in calcific aortic valve disease. *Biomed Pharmacother.* 2024;178:117143.
50. Hall IF, Kishta F, Xu Y, Baker AH, Kovacic JC. Endothelial to mesenchymal transition: at the axis of cardiovascular health and disease. *Cardiovasc Res.* 2024;120:223–36.
51. Zanotti S, Canalis E. Notch Signaling and the Skeleton. *Endocr Rev.* 2016;37:223–53.
52. Canalis E. Notch in skeletal physiology and disease. *Osteoporos Int.* 2018;29:2611–21.
53. Zieba JT, Chen Y-T, Lee BH, Bae Y. Notch signaling in skeletal development, Homeostasis and Pathogenesis. *Biomolecules.* 2020;10:332.
54. Canalis E, Parker K, Feng JQ, Zanotti S. Osteoblast lineage-specific effects of Notch activation in the Skeleton. *Endocrinology.* 2013;154:623–34.
55. Ji Y, Ke Y, Gao S. Intermittent activation of notch signaling promotes bone formation. *Am J Transl Res.* 2017;9:2933–44.
56. Hilton MJ, Tu X, Wu X, Bai S, Zhao H, Kobayashi T, et al. Notch signaling maintains bone marrow mesenchymal progenitors by suppressing osteoblast differentiation. *Nat Med.* 2008;14:306–14.
57. Ramasamy SK, Kusumbe AP, Schiller M, Zeuschner D, Bixel MG, Milia C, et al. Blood flow controls bone vascular function and osteogenesis. *Nat Commun.* 2016;7:13601.
58. Garg V, Muth AN, Ransom JF, Schluterman MK, Barnes R, King IN, et al. Mutations in NOTCH1 cause aortic valve disease. *Nature.* 2005;437:270–4.
59. Majumdar U, Manivannan S, Basu M, Ueyama Y, Blaser MC, Cameron E et al. Nitric oxide prevents aortic valve calcification by S-nitrosylation of USP9X to activate NOTCH signaling. *Sci Adv.* 2021;7.
60. Kostina A, Semenova D, Kostina D, Uspensky V, Kostareva A, Malashicheva A. Human aortic endothelial cells have osteogenic notch-dependent properties in co-culture with aortic smooth muscle cells. *Biochem Biophys Res Commun.* 2019;514:462–8.
61. Lin MI, Price EN, Boatman S, Hagedorn EJ, Trompouki E, Satischandran S et al. Angiopoietin-like proteins stimulate HSPC development through interaction with notch receptor signaling. *Elife.* 2015;4.
62. Denzer L, Muranyi W, Schrotten H, Schwerk C. The role of PLVAP in endothelial cells. *Cell Tissue Res.* 2023;392:393–412.
63. Swaminathan B, Youn S-W, Naiche LA, Du J, Villa SR, Metz JB, et al. Endothelial notch signaling directly regulates the small GTPase RND1 to facilitate notch suppression of endothelial migration. *Sci Rep.* 2022;12:1655.
64. Lilly B, Kennard S. Differential gene expression in a coculture model of angiogenesis reveals modulation of select pathways and a role for notch signaling. *Physiol Genomics.* 2009;36:69–78.
65. Gorski B, Liu F, Ma X, Chico TJA, Shrinivasan A, Kramer KL, et al. The heparan sulfate editing enzyme Sulf1 plays a novel role in zebrafish VegfA mediated arterial venous identity. *Angiogenesis.* 2014;17:77–91.
66. Zhao N, Liu H, Lilly B. Reciprocal regulation of Syndecan-2 and Notch Signaling in Vascular smooth muscle cells. *J Biol Chem.* 2012;287:16111–20.
67. Meyers JR, Planamento J, Ebrom P, Krulowitz N, Wade E, Pownall ME. Sulf1 modulates BMP signaling and is required for somite morphogenesis and development of the horizontal myoseptum. *Dev Biol.* 2013;378:107–21.
68. Ciumas M, Eyries M, Poirier O, Maugeenre S, Dierick F, Gambaryan N, et al. Bone morphogenetic proteins protect pulmonary microvascular endothelial cells from apoptosis by upregulating α -B-Crystallin. *Arterioscler Thromb Vasc Biol.* 2013;33:2577–84.
69. Tian B, Li X, Li W, Shi Z, He X, Wang S, et al. CRYAB suppresses ferroptosis and promotes osteogenic differentiation of human bone marrow stem cells via binding and stabilizing FTH1. *Aging.* 2024;16:8965–79.
70. Zhu B, Xue F, Li G, Zhang C. CRYAB promotes osteogenic differentiation of human bone marrow stem cells via stabilizing β -catenin and promoting the wnt signalling. *Cell Prolif.* 2020;53.
71. Wang Z, Chen C, Sun L, He M, Huang T, Zheng J, et al. Fibroblast growth factor 2 promotes osteo/odontogenic differentiation in stem cells from the apical papilla by inhibiting PI3K/AKT pathway. *Sci Rep.* 2024;14:19354.
72. Fei Y, Xiao L, Doetschman T, Coffin DJ, Hurley MM. Fibroblast growth factor 2 stimulation of osteoblast differentiation and bone formation is mediated by modulation of the wnt signaling pathway. *J Biol Chem.* 2011;286:40575–83.
73. Byun MR, Kim AR, Hwang J-H, Kim KM, Hwang ES, Hong J-H. FGF2 stimulates osteogenic differentiation through ERK induced TAZ expression. *Bone.* 2014;58:72–80.
74. Pielies O, Reck A, Morszczek C. High endogenous expression of parathyroid hormone-related protein (PTHrP) supports osteogenic differentiation in human dental follicle cells. *Histochem Cell Biol.* 2020;154:397–403.
75. Vadana M, Cecoltan S, Ciortan L, Macarie RD, Mihaila AC, Tucureanu MM, et al. Parathyroid hormone induces human valvular endothelial cells dysfunction

- that impacts the osteogenic phenotype of valvular interstitial cells. *Int J Mol Sci.* 2022;23:3776.
76. Rashid G, Bernheim J, Green J, Benchetrit S. Parathyroid hormone stimulates endothelial expression of atherosclerotic parameters through protein kinase pathways. *Am J Physiology-Renal Physiol.* 2007;292:F1215–8.
 77. Hyun J, Lee M, Rehman J, Pajcini KV, Malik AB. Notch1 promotes ordered revascularization through Semaphorin 3 g modulation of downstream vascular patterning signalling factors. *J Physiol.* 2022;600:509–30.
 78. Wagley Y, Chesni A, Acevedo PK, Lu S, Wells AD, Johnson ME, et al. Canonical notch signaling is required for bone morphogenetic protein-mediated human osteoblast differentiation. *Stem Cells.* 2020;38:1332–47.
 79. Cao J, Wei Y, Lian J, Yang L, Zhang X, Xie J, et al. Notch signaling pathway promotes osteogenic differentiation of mesenchymal stem cells by enhancing BMP9/Smad signaling. *Int J Mol Med.* 2017;40:378–88.
 80. Wu M, Chen G, Li Y-P. TGF- β and BMP signaling in osteoblast, skeletal development, and bone formation, homeostasis and disease. *Bone Res.* 2016;4:16009.
 81. Bonilla-Claudio M, Wang J, Bai Y, Klysiak E, Selever J, Martin JF. Bmp signaling regulates a dose-dependent transcriptional program to control facial skeletal development. *Development.* 2012;139:709–19.
 82. Cen X, Pan X, Zhang B, Huang W, Pei F, Luo T, et al. miR-20a-5p contributes to osteogenic differentiation of human dental pulp stem cells by regulating BAMBI and activating the phosphorylation of Smad5 and p38. *Stem Cell Res Ther.* 2021;12:421.
 83. Wu J, Chen X, Sehgal P, Zhang T, Jackson-Weaver O, Gou Y, et al. Arginine methylation of R81 in Smad6 confines BMP-induced Smad1 signaling. *J Biol Chem.* 2021;296:100496.
 84. Yano M, Inoue Y, Tobimatsu T, Hendy GN, Canaff L, Sugimoto T, et al. Smad7 inhibits differentiation and mineralization of mouse osteoblastic cells. *Endocr J.* 2012;59:653–62.
 85. Xiao F, Wang C, Wang C, Gao Y, Zhang X, Chen X. BMPER enhances bone formation by promoting the osteogenesis-angiogenesis coupling process in mesenchymal stem cells. *Cell Physiol Biochem.* 2018;45:1927–39.
 86. Zhang J, Ma Z, Yan K, Wang Y, Yang Y, Wu X. Matrix gla protein promotes the bone formation by Up-Regulating Wnt/ β -Catenin signaling pathway. *Front Endocrinol (Lausanne).* 2019;10.
 87. Kim S, Koga T, Isobe M, Kern BE, Yokochi T, Chin YE, et al. Stat1 functions as a cytoplasmic attenuator of Runx2 in the transcriptional program of osteoblast differentiation. *Genes Dev.* 2003;17:1979–91.
 88. Tajima K, Takaishi H, Takito J, Tohmonda T, Yoda M, Ota N, et al. Inhibition of STAT1 accelerates bone fracture healing. *J Orthop Res.* 2010;28:937–41.
 89. Zhang Y, Jing Z, Cao X, Wei Q, He W, Zhang N, et al. SOCS1, the feedback regulator of STAT1/3, inhibits the osteogenic differentiation of rat bone marrow mesenchymal stem cells. *Gene.* 2022;821:146190.
 90. Takayanagi H, Kim S, Koga T, Taniguchi T. Stat1-mediated cytoplasmic attenuation in osteoimmunology. *J Cell Biochem.* 2005;94:232–40.
 91. Nascimento HM, Pelegrino MT, Pieretti MC, Seabra JB. How can nitric oxide help osteogenesis? *AIMS Mol Sci.* 2020;7:29–48.
 92. Cooke JP, Losordo DW. Nitric oxide and angiogenesis. *Circulation.* 2002;105:2133–5.
 93. Won J, Kim WJ, Shim JS, Ryu JJ. Guided bone regeneration with a nitric-oxide releasing polymer inducing angiogenesis and Osteogenesis in critical-sized bone defects. *Macromol Biosci.* 2022;22.
 94. Veeriah V, Zanniti A, Paone R, Chatterjee S, Rucci N, Teti A, et al. Interleukin-1 β , lipocalin 2 and nitric oxide synthase 2 are mechano-responsive mediators of mouse and human endothelial cell-osteoblast crosstalk. *Sci Rep.* 2016;6:29880.
 95. Bosse K, Hans CP, Zhao N, Koenig SN, Huang N, Guggilam A, et al. Endothelial nitric oxide signaling regulates Notch1 in aortic valve disease. *J Mol Cell Cardiol.* 2013;60:27–35.

Publisher's note

Springer Nature remains neutral with regard to jurisdictional claims in published maps and institutional affiliations.